Eighth International Conference on
THIN-WALLED STRUCTURES – ICTWS 2018
Lisbon, Portugal, July 24-27, 2018

ON THE BUCKLING BEHAVIOR OF RING-STIFFENED SHELLS UNDER AXIAL COMPRESSION

Andreas Jäger-Cañás*, Hartmut Pasternak**

* EHS beratende Ingenieure für Bauwesen GmbH (external PhD student at BTU), Lohfelden, Germany
e-mail: a.jaeger_ehs@t-online.de

** BTU, Chair of Steel and Timber Construction, Cottbus, Germany
e-mail: Hartmut.Pasternak@b-tu.de

Keywords: Axial buckling; ring stiffening; shell; stability.

Abstract. *Extensive studies on ring-stiffened, cylindrical shells subject to uniform axial compression were conducted in the 1960s and 1970s. The stiffeners' beneficial effect on the axial buckling behavior was well recognized. However, standards for typical civil engineering structures do not provide detailed rules that allow to take into account the increased buckling capacity. With the trend towards more sustainable structures, the use of very thin-walled structures, which are prone to axial buckling, became more common and improved rules for the axial buckling check became necessary to allow for economic designs. In this paper, one approach to predict the buckling resistance of ring-stiffened shells under axial compression is presented. The proposed procedure allows the determination of failure loads of closely and widely stiffened shells. The provided rules are directly applicable to any typical civil engineering structure that buckles elastically.*

1 INTRODUCTION

Cylindrical shells are well known for their structural efficiency, especially when they are subject to uniform axial compression. Their behavior has been studied since the early 1900s with major progress in the understanding of shell behavior and the prediction of failure loads.

With the increasing demand of faster, stronger and more light-weight structures, stiffened shells became more important. While first, ring-stiffened shells promised to satisfy the demands of ship and airplane builders, the availability of new construction methods motivated a development of more complex structures, consequently leading to grid-stiffened shells.

Until today, ring-stiffened shells in civil engineering were employed, primarily to withstand external pressure and wind. The beneficial behavior regarding axial compression has hardly been recognized.

Figure 1: Closely ring-stiffened cylinder (l., [1]) and widely ring-stiffened tank (r., [2])

The trend towards increased sustainability resulted in more light-weight structures with a highly efficient use of material becoming necessary. As was found out in the late 1960s, ring stiffeners do not only enhance the circumferential buckling but as well have a significant effect on the meridional buckling behavior. Their ability to increase the failure load up to the critical load becomes especially interesting, when very light-weight cylindrical shells, such as biogas digesters or storage tanks are built. Their very thin strakes, reaching up to *r/t* (with *r* as the radius and *t* as the thickness of the shell) ratios of 10000 are prone to local buckling. Hence, it is vital to make use of the present stiffeners in the design process to allow for very efficient, more economical structures.

As a contribution to the ongoing trend towards more sustainable constructions in steel, this paper aims at providing a design procedure that allows to take into account the increased buckling resistance due to the influence of ring-stiffeners.

A formulation of the elastic imperfection reduction factor α, which relates the limit load derived by a geometrically and physically nonlinear analysis with imperfections included (GMNIA) to the bifurcation load (LBA) is proposed. The formulae presented are valid for the parameter range of $500 \leq r/t \leq 10000$, in which elastic buckling is anticipated.

Since unstiffened cylindrical shells are often treated too conservatively, a proposal is made that allows to take into account the lower bound value observed from experiments.

A design rule for closely ring-stiffened shells is presented that makes an evaluation of the bearing capacity related to the characteristic imperfection amplitude possible. As the last step, a correction factor is proposed that extends the design procedure on widely stiffened shells, allowing to evaluate stiffened shells with typical civil engineering structures' parameters.

2 UNSTIFFENED SHELLS

Unstiffened shells subject to axial compression again gained closer attention when *Rotter* [3] used the modified capacity curve for the extraction of the buckling curve parameters. His proposal for the determination of the elastic imperfection reduction factor (knockdown factor) α has been adopted almost unchanged in the current standards, e.g. EN 1993-1-6:2017 [4].

Unfortunately, the equation (eq. 1) for the calculation of α has been approximated in a range of the imperfection depth that is typical for shells with a *r/t* ratio of about 1000 for fabrication quality class C (FQC C). Consequently, the bearing capacity of more thin-walled shells are predicted conservatively, e.g. $r/t = 10000$: $\alpha = 0.083$.

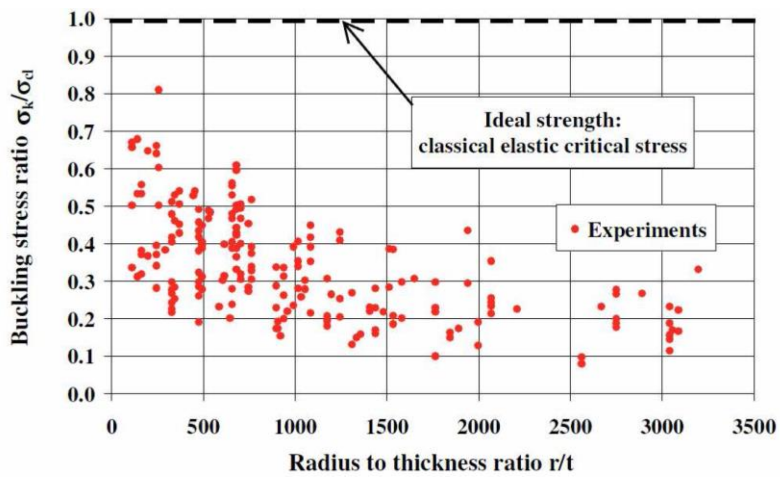

Figure 2: Experimental strength of isotropic axially compressed cylinders [6]

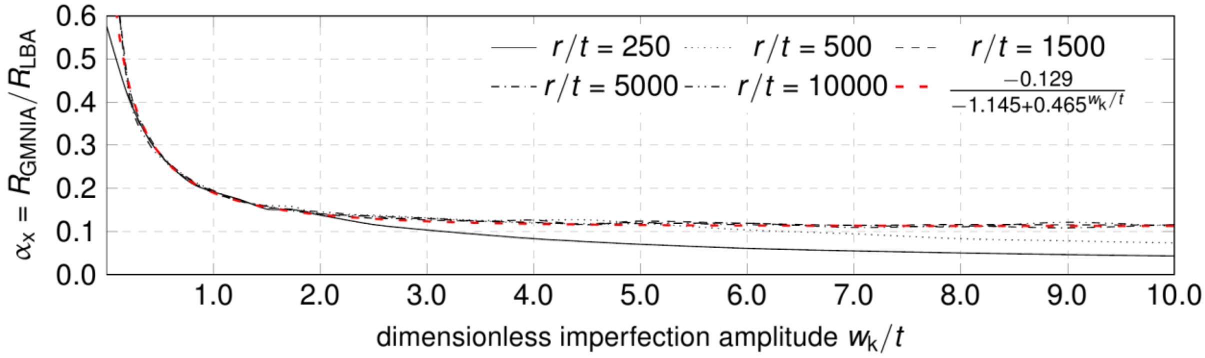

Figure 3: Lower bound of numerically derived knockdown factors α dependent on $\Delta w_k/t$ [8]

$$\frac{\Delta w_k}{t} = \frac{1}{Q}\sqrt{\frac{r}{t}} \qquad \text{With: } \begin{array}{l} Q = 16 \text{ (FQC C)} \\ Q = 25 \text{ (FQC B)} \\ Q = 40 \text{ (FQC A)} \end{array} \tag{1}$$

$$\alpha_x = \frac{0.83}{1 + 2.2\left(\frac{\Delta w_k}{t}\right)^{0.88}} \tag{2}$$

$$\alpha_{x,nst} = \frac{-0.129}{-1.145 + 0.465^{\Delta w_k/t}} \tag{3}$$

While this is a step forward, compared to the former EN 1993-1-6:2007 [5], still the capacity is lower than it may be expected from the experiments, e.g. [6] (fig. 2). A numerical study indicated that a lower bound value of α = 0.12 may be adopted into a design procedure [7]. As fig. 3 shows, *r/t* ratios higher or equal to 1000 allow for a unique expression of the knockdown factor (indexed with “nst” for non-stiffened) given by eq. 3.

The imperfection amplitude according to eq. 1 may be halved when eq. 3 is employed. The curve shown in fig. 3 was deduced using an eigenform affine ring buckle as imperfection. Inward and outward deviations exist that do not allow a direct interpretation in terms of tolerance measurements, where usually only outward deflections are present. Therefore, the imperfection shape has to be interpreted as if it was shifted off the meridian by one half-wave, yielding twice the amplitude of, e.g. a weld imperfection.

3 CLOSELY RING-STIFFENED SHELLS

3.1 Experiments

A collection of many experiments conducted on ring-stiffened shells subject to axial compression [9] were reviewed to derive a simple lower bound criterion for the determination of the knockdown factor in dependence of the ring parameter k_{st} (eq. 4) [10]. An optimized formulation was published in [8], which is denoted as eq. 5 and depicted in fig. 4 as dashed line (“αrst” with “rst” indicating ring stiffening).

$$k_{st} = \frac{A_{st}}{a_{st}\, t} \tag{4}$$

Where: A_{st} = stiffener’s cross-sectional area, a_{st} = stiffener spacing, t = thickness of the shell

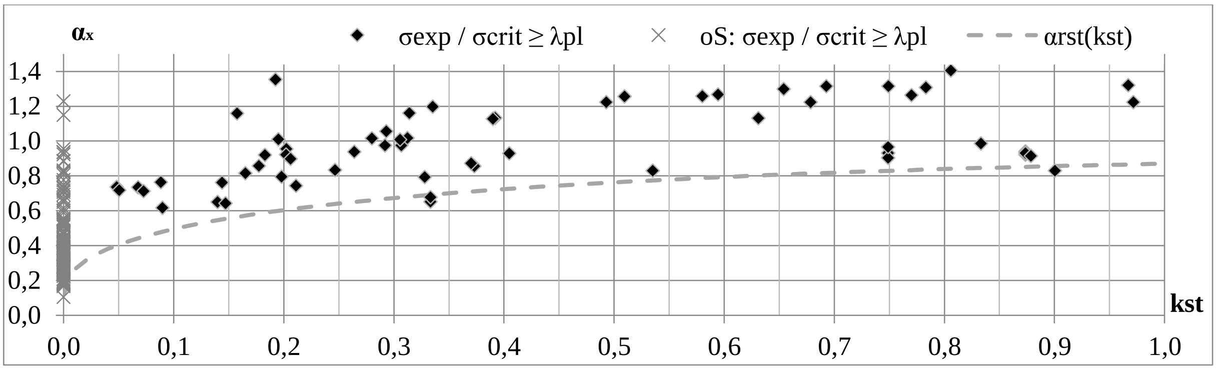

Figure 4: Knockdown factor only depending on the ring parameter

$$\alpha_{x,rst}(k_{\mathrm{st}}) = \sqrt{k_{\mathrm{st}}}\,(1.7 - k_{\mathrm{st}}^{0.25})\,\left(0.9 + 2\cdot 10^{-5}\frac{r}{t}\,k_{\mathrm{st}}\right) \tag{5}$$

$$l_{BHW} = 1.73\,\sqrt{rt} \tag{6}$$

Since most of the experiments were carried out employing a stiffener spacing of less than two buckling half wave lengths (BHW, eq. 6), they are referred to as "closely spaced".

Typically, the load bearing behavior is heavily influenced by the stiffeners that may remarkably reduce the imperfection sensitivity by subdividing the shell into short sub shells. Additionally, meridional clamping moments develop due to the prevented circumferential extension in the vicinity of the stiffeners. Lateral contraction is more pronounced as the stiffeners' cross section is increased, consequently leading to higher clamping degrees at the stiffeners. As can be interpreted from fig. 4, these effects occur even at low degrees of ring-stiffening. Where the lower bound of test results allows the conclusion of $\alpha_x = 0.6$ when k_{st} is 0.1, which is five times larger than the lower bound of unstiffened shells. An additional strength gain until $k_{st} = 1.0$ of about 33 % is possible.

While a positive effect on elastic buckling is observable, the opposite may be true for thick-walled shells that fail in the elastic-plastic range. Due to the meridional bending moments, early yielding may occur, resulting in a reduction of the buckling capacity.

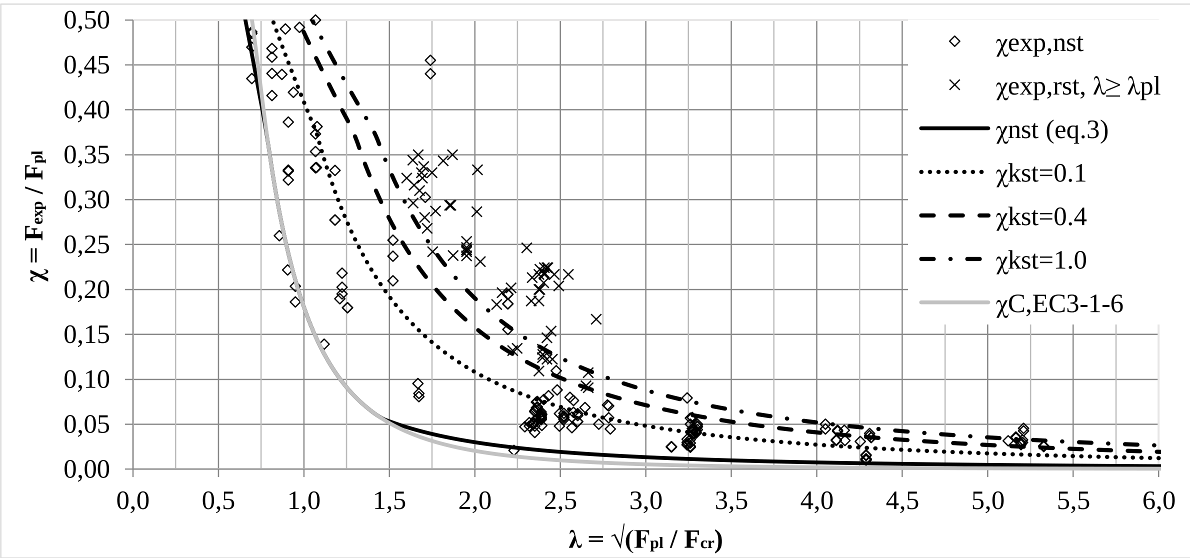

Figure 5: Buckling curve for unstiffened and ring-stiffened shells for FQC C

The evaluation in terms of a buckling curve is presented in fig. 5. Experimental values are plotted as “χexp,nst ” for unstiffened shells and with “χexp,rst” when ring stiffeners are attached. The higher resistance of unstiffened shells is visible for very slender shells when a lower bound for α_x (“χnst” with $\alpha \geq 0.12$), is adopted. The curve named “χC,EC3-1-6” shows the regular shape according to eq. 2 without a lower bound for α_x. Obviously, even small ring stiffeners are sufficient to incredibly raise the buckling capacity.

3.2 Numerical calculations

The trend of describing the behavior of shells not only via lower bounds of experiments but more differentiated, in terms of imperfection measurements, was the motivation to develop a design concept that is compatible with the current Eurocode [4] design approach.

The study aimed at describing ring-stiffened shells with *r/t* ratios between 500 up to 10000, consisting of ring parameters k_{st} of 0.1 up to 1.0. The results were obtained employing the Sofistik software suite [11]. Using eigenform affine ring buckles, a quasi-static, dynamically stabilized analysis was carried out that was succeeded by the determination of critical buckling loads along the load-deflection path in intervals of four load steps. A bisection of the interval was carried out when the accompanied determined eigenvalues sunk below unity and the result was saved. When all accompanying eigenvalues were above unity, a static Newton-Raphson analysis was used for comparison with the quasi-static approach. The minimum of both analysis was then stored as the result.

Thin shells benefit more, even from light stiffening, than thicker shells. As can be seen in fig. 6, the shape of the curve looks very similar to that of an unstiffened shell (fig. 3) with a huge loss of capacity at small imperfection depths. The ring stiffeners do not alter the behavior much. Contrary, directly visible in fig. 7, the behavior is completely changed for thin-walled shells, especially for higher ring parameters. While the effect of stiffening is small for *r/t* = 500, with *r/t* = 5000 even small changes in the ring parameter lead to a different outcome of the numerical calculation.

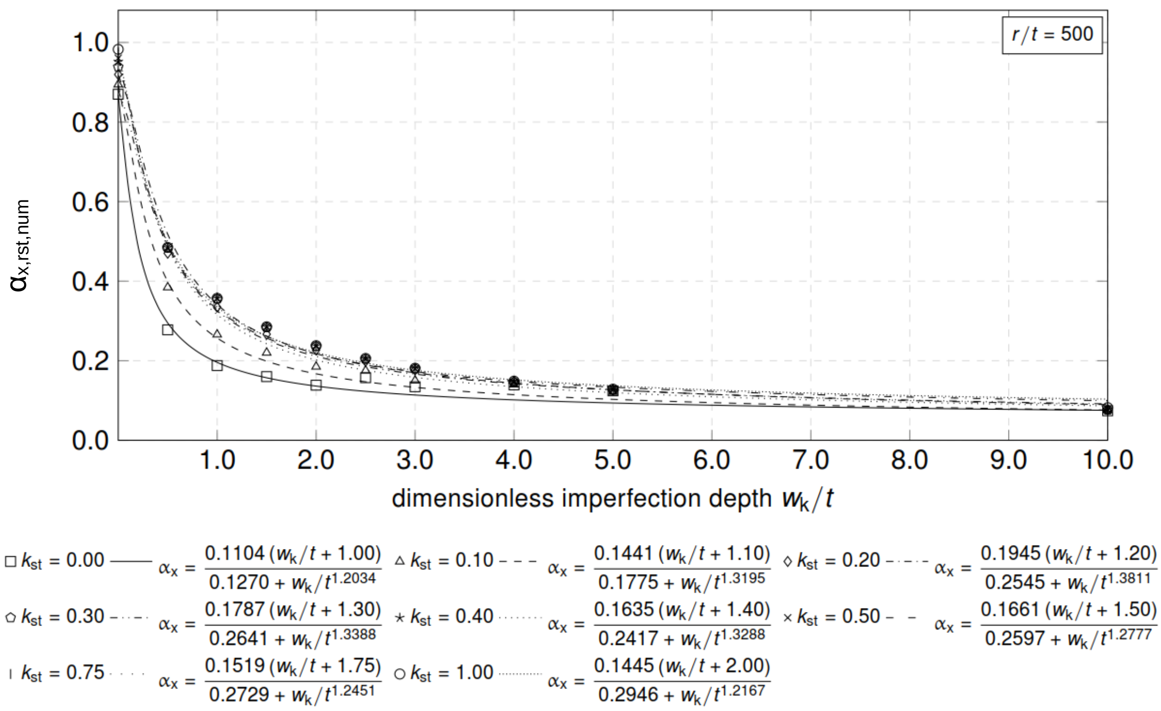

Figure 6: Knockdown factor depending on *w/t* of closely ring-stiffened shells with *r/t* = 500

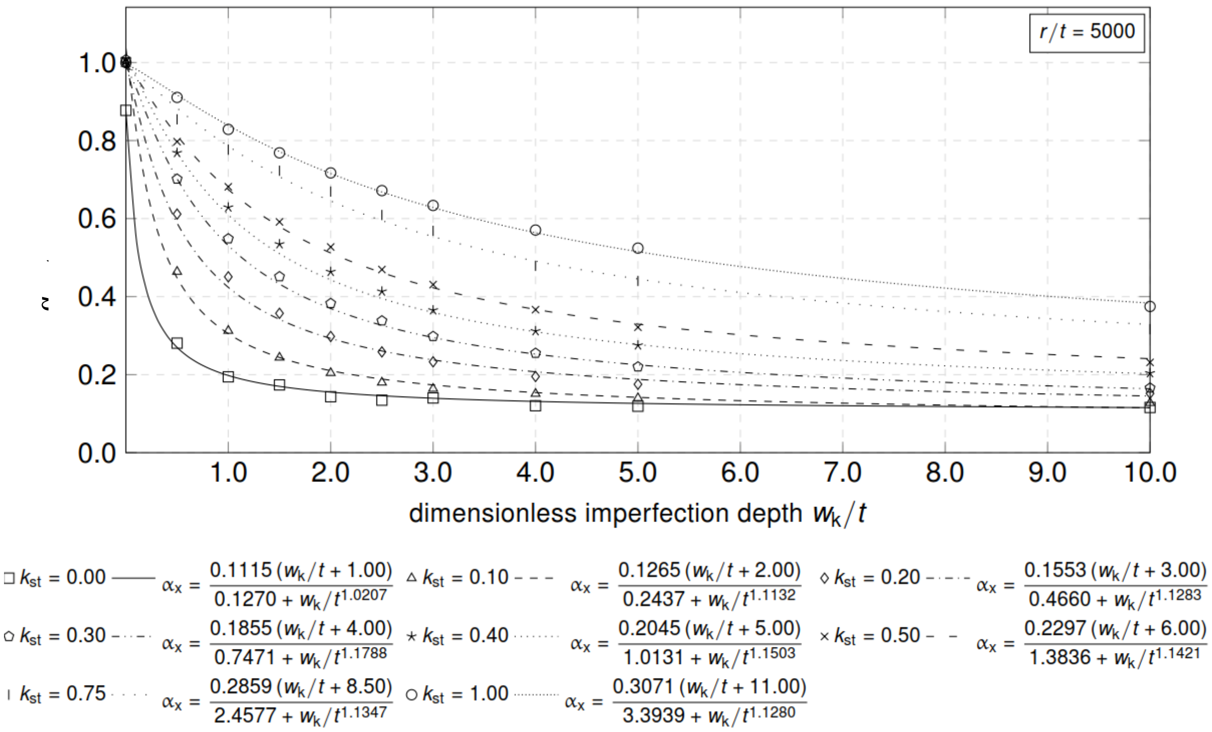

Figure 7: Knockdown factor depending on *w/t* of closely ring-stiffened shells with *r/t* = 5000

It is this difference in the behaviors of different parameter combinations that make the interpolation of the numerical results a challenge. The resistance is not only influenced by the ring parameter, but as well by the *r/t* ratio and the imperfection amplitude. Some simplifications are necessary to be able to capture the specific features of all parameter combinations and allow the deduction of a hand calculation procedure.

In figs. 6 and 7, already the approach to interpolate the results is presented in the legend. A close representation of the curves depending on the imperfection amplitude that furthermore result in values easy to approximate over the ring parameter, is found with eq. 7. Due to the ring stiffening, the geometric nonlinearity effects are reduced, which allows for a more optimistic determination of α_g in dependence of the ring parameter (denoted as $\alpha_{g,rst}$) compared to the proposal in [4].

$$\alpha_{x,nst} \leq \alpha_{x,rst,cal} = \frac{\left(1 + \frac{w}{t} + \frac{k_{st}}{500}\frac{r}{t}\right) x}{y + \left(\frac{w}{t}\right)^{z}} \leq 0.9 + \frac{k_{st}}{10} = \alpha_{x,g.rst} \tag{7}$$

The parameters *x*, *y* and *z* are slightly closer interpolated over k_{st} when they are multiplied with the according value of k_{st} as proposed with eqs. 8a-c. Since minor deviations from the actual parameters *x*, *y* and *z* may result in large errors in $\alpha_{rst,cal}$, this modification is preferred over the unmodified interpolation. Examples are given for *r/t* = 500 and *r/t* = 5000 in figs. 8 and 9.

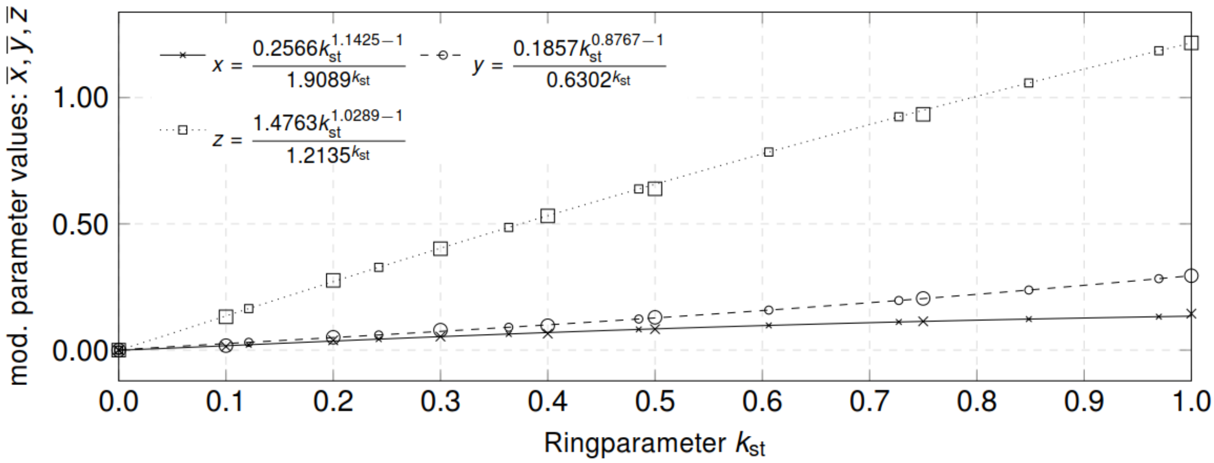

Figure 8: Interpolation of the modified approximated values over the ring parameter, *r/t* = 500

$$\bar{x}\, k_{st} \rightarrow x = \frac{x_a\, k_{st}^{x_b - 1}}{x_c^{k_{st}}} \tag{8a}$$

$$\bar{y}\, k_{st} \rightarrow y = \frac{y_a\, k_{st}^{y_b - 1}}{y_c^{k_{st}}} \tag{8b}$$

$$\bar{z}\, k_{st} \rightarrow z = \frac{z_a\, k_{st}^{z_b - 1}}{z_c^{k_{st}}} \tag{8c}$$

A further interpolation of the parameters x_a to z_c over *r/t* would need quite accurate descriptions of the curve shapes because even small errors would significantly alter the result of $\alpha_{rst,num}$. Therefore, it is recommended to linearly interpolate between adjacent *r/t* ratios, or simplified, use the set of parameters of the lower *r/t* ratio given in table 1, to determine the knockdown factor.

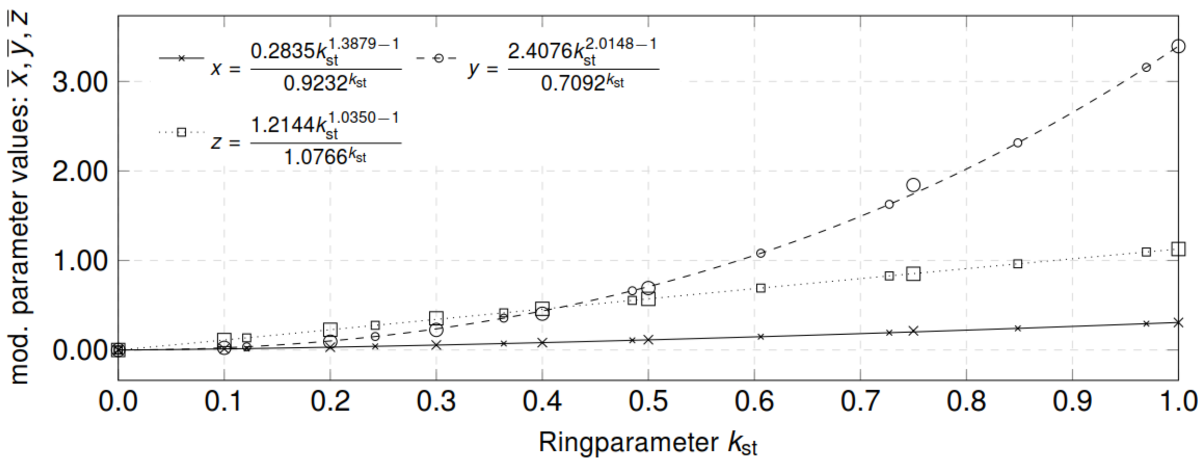

Figure 9: Interpolation of the modified approximated values over the ring parameter, *r/t* = 5000

Table 1: Parameters for the determination of the knockdown factor of closely ring-stiffened shells

r/t	500	1000	1500	2000	2500	5000	7500	10000
x_a	0.257	0.651	0.796	0.739	0.504	0.284	0.243	0.211
x_b	1.143	1.616	1.763	1.756	1.585	1.388	1.346	1.294
x_c	1.909	3.283	3.338	2.562	1.707	0.923	1.052	1.060
y_a	0.186	1.423	3.973	3.713	3.164	2.408	5.579	4.170
y_b	0.877	1.921	2.441	2.462	2.311	2.015	2.343	2.141
y_c	0.630	2.396	4.097	2.441	1.796	0.709	1.446	1.004
z_a	1.476	2.184	1.523	1.475	1.641	1.214	1.606	1.327
z_b	1.029	1.284	1.145	1.129	1.180	1.035	1.166	1.079
z_c	1.214	1.836	1.282	1.189	1.360	1.077	1.544	1.336

The interpolation procedure has been verified by comparing the numerical result with the approximation (fig. 10). While for r/t = 500 a huge overestimation seems to be calculated, for all other geometries the range of values is between 0.9 times up to 1.3 times the target value. When the material safety factor γ_{M1} = 1.1 is considered, all results are safe and quite close to the numerical calculations. Considering r/t = 500, it is evident from fig. 6 that, at high imperfection amplitudes, α_x is overestimated. However, since the typical imperfection depth according to eq. 1 is about 1.4 t for FQC C, the unsafe prediction at higher imperfection depths is negligible. The same is true for r/t = 1000 and 1500 (fig. 10), where two results seem to be unsafe, which is not true, provided the correct imperfection amplitude is considered.

A simplification is possible as indicated in fig. 11 (at the example of $\Delta w_k/t$ = 0.5 (red line) and $\Delta w_k/t$ = 3.0 (blue line). The reduction factor may be determined in specific intervals that depend on r/t and k_{st}. When k_{st} is less than 0.4, a straight line interpolation between α_{nst} and α_{rst} at r/t = 1000, then between r/t = 1000 and r/t = 10000 is justifiable. If the ring parameter exceeds 0.4, the linear interpolation shall be carried out using r/t = 2000 instead of r/t = 1000.

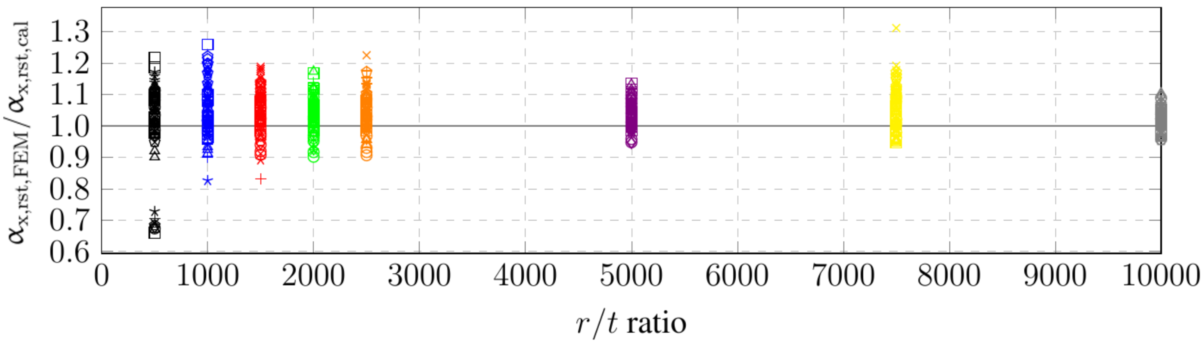

Figure 10: Verification of the approximation of numerical results of closely ring-stiffened shells

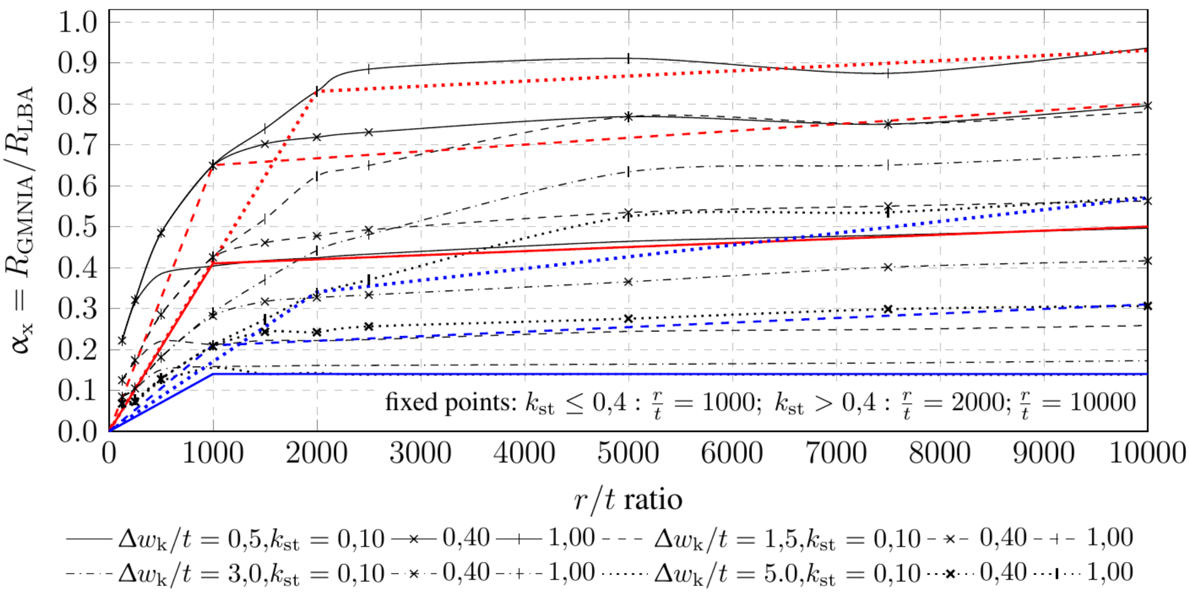

Figure 11: Interpolation of the modified approximated values over the ring parameter, *r/t* = 5000

4 RING-STIFFENED SHELLS WITH ARBITRARY STIFFENER SPACING

Typical structures in civil engineering are built with wide stiffener spacing due to reduction of erection costs. With an increasing distance between two ring stiffeners, their beneficial effect vanishes and the bearing capacity drops to a value as low as for an unstiffened shell. Especially light-weight structures with very high *r/t* ratios suffer from even small axial forces so that it is of high interest for designers to take advantage of the present stiffeners as much as possible.

To overcome the limitation of the current standard [4], a further parametric study has been conducted dealing specifically with the axial buckling behavior of cylindrical shells with widely spaced ring-stiffeners. Tanks and silos with distances of ring stiffeners that exceed two buckling half-wave lengths (eq. 6) are considered as “widely stiffened”.

The range of parameters included *r/t* ratios of 500, 1000, 1500, 2500 and 5000. If *r/t* less than 500 is considered, the shell should be treated as unstiffened. If this ratio exceeds 5000, a maximum of 5000 shall be assumed for *r/t* to yield safe results.

The ring parameter k_{st} was evaluated at 0.1, 0.2, 0.4 and 1.0 in the range of imperfection depths $\Delta w_k/t$ between 0 and 10.

The stiffener spacing $\overline{a_{st}}$ (eq. 9) was chosen as multiples of the buckling half-wave length: 1, 2, 2.5, 3, 3.5, 5, 7.5, 10 and 15 (while 15 is used for the unstiffened shell).

$$\overline{a_{st}} = \frac{a_{st}}{1.73\sqrt{rt}} \quad (9)$$

A direct interpolation of the numerical results was not considered due to the complexity. While a result for the closely stiffened shell should be available already, it seemed to be best practice to determine a factor as given in eq. 10 that allows to take into account any stiffener spacing. It was expected that partially quite conservative results would be determined because a lower bound curve for every ring parameter determined from all *r/t* ratios and all imperfection depths was used to approximate the factorized knockdown factor safely.

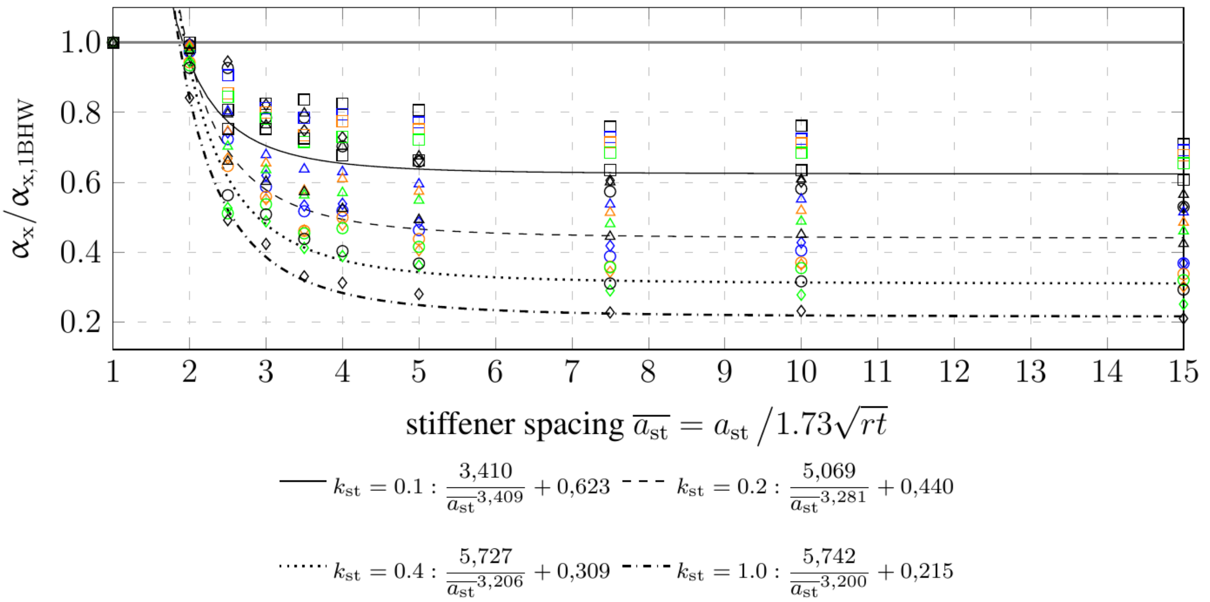

Figure 12: Factorized knockdown factor depending on the ring parameter and stiffener spacing

$$k_{\alpha,\mathrm{rst}} = \left(a\,\overline{a_{\mathrm{st}}}^{\,-b} + c\right) k_{\mathrm{rst}} \leq 1 \tag{10a}$$

with:

$$a = 5.999 - \frac{0.257}{k_{\mathrm{st}}} \tag{10b}$$

$$b = 3.177 - \frac{0.023}{k_{\mathrm{st}}} \tag{10c}$$

$$c = 0.169 - \frac{0.046}{k_{\mathrm{st}}} \tag{10d}$$

The lower bound curves are depicted in fig. 12, providing the equations for the according curves. The dependence on the ring parameter can be approximated using eqs. 10a-d.

It was observed that the lowest values for k_α were reached at the highest *r/t* ratio considered. Since especially very thin-walled shells gain buckling strength when ring-stiffeners are attached, the absence of stiffeners consequently causes a huge reduction in bearing capacity.

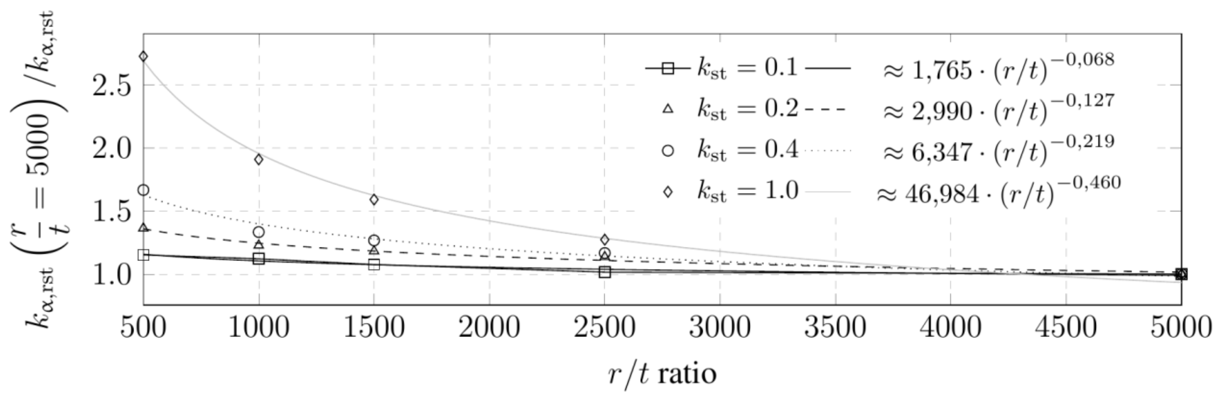

Figure 13: Dependence of the factorized knockdown factor from *r/t* and k_{st}

To allow for less conservatism, a factor was deduced that takes into account that at lower *r/t* ratios the loss iof strength is less pronounced. At $\overline{a_{\mathrm{st}}} \geq 5$ the factors of $\alpha_{x,rst}$ for *r/t* = 5000 to the other *r/t* ratios were determined for each ring parameter. The result is depicted in fig. 13 and the approximation parameters are given with eqs. 11a-c. The parameters *x* and *y* relate on $k_{st.}$ The necessary interpolation depending on the ring parameter is given with eqs. 11b and 11c. Since the value of k_α is larger when the spacing is small, it was assumed that the influence of *r/t* vanishes as the stiffener spacing gets closer towards two buckling half-wave lengths. An iteratively optimized factor depending on $\overline{a_{\mathrm{st}}}$ was chosen with a limit of one for large distances between two adjacent stiffeners.

$$k_{\mathrm{rst}} = 1 + \left[i \left(\frac{r}{t}\right)^{k} - 1 \right] \min\left(1; \frac{\overline{a_{\mathrm{st}}}}{5}\right) \tag{11a}$$

with:

$$i = 1.568 \cdot 29.976^{k_{\mathrm{st}}} \tag{11b}$$

$$k = -0.427\, k_{\mathrm{st}} - 0.042 \tag{11c}$$

To verify the proposed procedure, the numerical calculations indicated as "$\alpha_{x,rst,FEM}$" in figs. 14 and 15 were compared with the calculated results ("$\alpha_{x,rst,cal}$"). Numerical results are approximated safely when the quotient exceeds unity. The larger this factor gets, the more conservative or uneconomical is the outcome of the calculation.

As can be seen in fig. 14, typically the interpolated results are quite conservative. Since a lower bound approach was employed, this outcome was expected. Unsafe predictions are found for closely stiffened shells and, drawn with black color, for almost all results of *r/t* = 500. While the results for *r/t* = 500 are easily explained with the large imperfection amplitudes for that unsafe results are predicted by the calculation procedure and, therefore those results are negligible, the other results require more detailed explanation.

Results only in the typical range of imperfection amplitudes, starting at about $\Delta w_k/t \approx 0.4$ (*r/t* = 500, FQC A reduced by a 25% safety margin) and reaching up to $\Delta w_k/t \approx 5.5$ (*r/t* = 5000, FQC C with a 25% safety margin) are depicted in fig. 15. It is shown that unsafe predictions of FEM results are in the range of the material safety factor $\gamma_{M1} = 1.1$.

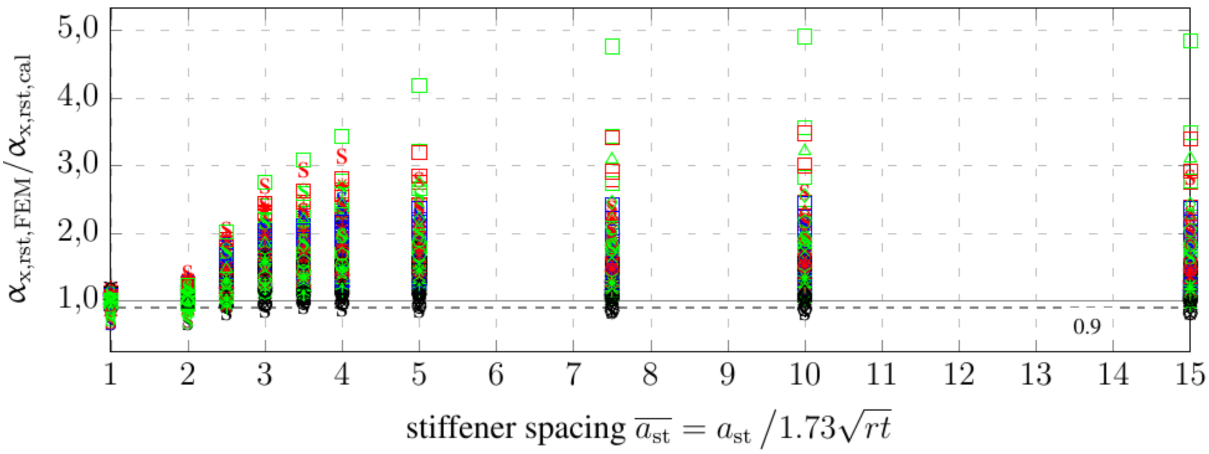

Figure 14: Verification of the proposed procedure – all results

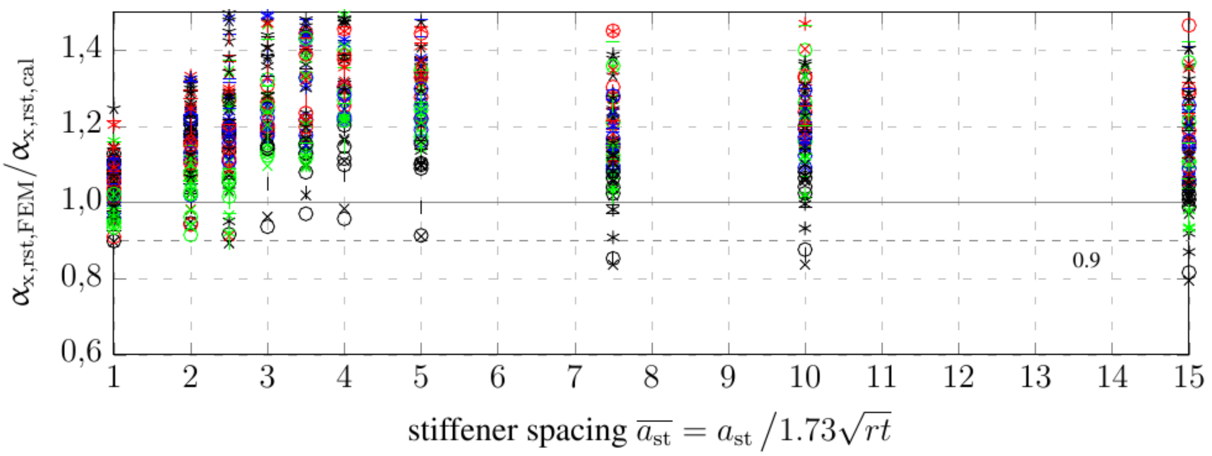

Figure 15: Verification of the proposed procedure – unrealistic results excluded

Black markers, indicating results of r/t = 500, may be neglected since imperfection depths exceeding $\Delta w_k/t \approx 2.0$ are unrealistic in construction practice.

5 CONCLUSION

For many years, the efficiency of ring-stiffened cylindrical shells subject to meridional compression has not been recognized in civil engineering practice. However, the trend towards more sustainability consequently lead to light-weight structures that are prone to failure due to axial buckling. To overcome the drawback of an uneconomical treatment set by present design codes, an improved design procedure was proposed that allows to take into account the beneficial effect of ring-stiffeners when tanks or silos are loaded by uniform axial compression. The formulation was derived by a numerical examination of closely stiffened shells and then extended to cylinders with wide stiffener spacing to allow a safe and economical applicability to all silos and tanks, which buckle in the elastic range.

6 REFERENCES

[1] Lipp GmbH. 2017

[2] Erich Stallkamp ESTA GmbH, *Tank der Firma Stallkamp*, Online, Available: https://www.stallkamp.de//images/produkte/behaelter/glattstahlbehaelter/V2A_Beh%C3%A4lter_3455x755m__7.081m%C2%B3.jpg. [Accessed 28 01 2018].

[3] J.M. Rotter, “The elastic-plastic imperfection sensitivity of axially compressed cylinders with weld depressions*”, EUROSTEEL 2008 - Proceedings of the 5th European Conference on Steel and Composite Structures*, Robert Ofner, Darko Beg, Josef Fink, Richard Greiner and Harald Unterweger (eds.), ECCS, Graz, 1497-1502, 2008.

[4] *EN 1993-1-6:2017 Eurocode 3: Design of steel structures - Part 1-6: Strength and stability of shell structures*, CEN, Brussels, 2017.

[5] *EN 1993-1-6:2007 Eurocode 3: Design of steel structures - Part 1-6: Strength and stability of shell structures*, CEN, Brussels, 2010.

[6] L. Harris, H. Suer, W. Skene and R. Benjamin, *The Stability of Thin-Walled Unstiffened Circular Cylinders under Axial Compression including the Effects of Internal Pressure, Journal of Aeronautical Sciences,* **24**(8), 587-596, 1957.

[7] A. Jäger-Cañás and H. Pasternak, „On the axial buckling of very thin-walled cylindrical shells“, *8th European Conference on Steel and Composite Structures (EUROSTEEL 2017),* Ernst & Sohn, Copenhagen, 1(2-3), 868-877, 2017.

[8] A. Jäger-Cañás and H. Pasternak, „Über das Tragverhalten ringversteifter Kreiszylinderschalen unter Axialdruck“, *DASt-Kolloqium 2018,* Kaiserslautern, 2018. (in print)

[9] S. Barlag, *Zur Modellbildung für numerische Stabilitätsuntersuchungen elastoplastisch versagender Kreiszylinder aus Stahl,* Dissertation, Hannover: University of Hannover, 2003.

[10] A. Jäger-Cañás and H. Pasternak, "Influence of closely spaced ring-stiffeners on the axial buckling behavior of cylindrical shells", 8*th European Conference on Steel and Composite Structures (EUROSTEEL 2017),* Ernst & Sohn, *C*openhagen, 1(2-3), 928-937, 2017.

[11] Sofistik, *VERiFiCATiON MANUAL*, HQ Oberschleissheim: Sofistik AG, 2013.